Feature Extraction with Intrinsic Distortion Correction in Celiac Disease Imagery: No Need for Rasterization

Michael Gadermayr[1], Andreas Uhl[1], and Andreas Vécsei[2]

[1] Department of Computer Sciences, University of Salzburg, Austria
{mgadermayr,uhl}@cosy.sbg.ac.at
http://www.wavelab.at
[2] St.Anna Children's Hospital, Endoscopy Unit, Vienna, Austria

Abstract. In the fields of computer aided celiac disease diagnosis, wide-angle endoscopy lenses are employed which introduce a significant degree of barrel type distortion. In recent studies on celiac disease classification, distortion correction techniques are investigated which use interpolation techniques, in order to maintain the rasterization of the image. Subsequent feature extraction is based on the new images. We introduce a generic feature extraction methodology with intrinsic distortion correction, which does not include this rasterization for features which do not need a regular grid. As distortion correction turned out to be disadvantageous in most cases, we aim in investigating the (negative) effect of the applied rasterization. In our experiments, the omission of rasterization actually turns out to be advantageous. This fact is an incentive for developing more features, which are not based on a regular grid.

1 Introduction

Celiac disease is an autoimmune disorder that affects the small bowel in genetically predisposed individuals of all age groups after introduction of gluten containing food. Characteristic for this disease is an inflammatory reaction in the mucosa of the small intestine caused by a dysregulated immune response triggered by ingested gluten proteins of certain cereals, especially against gliadine. During the course of the disease the mucosa looses its absorptive villi and hyperplasia of the enteric crypts occurs leading to a diminished ability to absorb nutrients. Computer aided celiac disease diagnosis relies on images taken during endoscopy. The employed cameras are equipped with wide angle lenses, which suffer from a significant amount of barrel type distortion. Whereas the distortion in central image pixels can be neglected, peripheral regions are highly distorted. Thereby, the feature extraction as well as the following classification is compromised. Based on camera calibration, distortion correction (DC) techniques are able to rectify the images.

In recent studies, the impact of barrel type distortion [1] and distortion correction [2] on the classification rate of celiac disease endoscopy images has been investigated. The authors showed that image patches in peripheral regions, which are stronger affected by the distortion are more likely to be misclassified. However, with distortion correction, the classification rate on average even suffers. In [3] and [4], different distortion correction techniques and in [5] additionally various interpolation methods have been investigated.

Applying traditional distortion correction introduces the following advantages (+) and disadvantages (–):

- **Geometrical correctness (+):**
  The geometrical relations are rectified.
- **Interpolation within rasterization (–):**
  As the mapping from distorted to undistorted points usually does not result in discrete points, interpolation is necessary.
- **Lack of data points in peripheral regions (–):**
  Due to the stretching of the image points, in peripheral regions, less real data points are available.

In this work, we introduce a generic method to extract distortion corrected features without the need of a previous rasterization. In order to measure the (negative) effect of interpolation in rasterization, the new approach is compared with the traditional feature extraction based on distortion corrected images. Moreover, we compare the new approach with the method based on distorted images which turned out to be mostly advantageous in recent work [2]. In experiments, the competitiveness of the new approach is confirmed. We have to point out, that the proposed approach requires features which are not based on a regular grid, as otherwise the advantage would vanish. In experiments, we show that the proposed intrinsic approach definitely is advantageous compared to the traditional approach based on DC images and for certain setups it is advantageous compared to the approach based on original images.

The paper is organized as follows: In Sect. 2, the traditional way of distortion corrected feature extraction and the new intrinsic technique is explained. In Sect. 3, experiments are shown and the results are discussed. Section 4 concludes this paper.

2 Theory

2.1 Distortion Model

We utilize the distortion correction approach based on the work of Melo et al. [6]. In this approach, the circular barrel type distortion is modeled by the division model [7]. Having the center of distortion $\hat{x}_c$ and the distortion parameter ξ, undistortion (DC) of distorted points x_d and distortion (D) of undistorted points x_u is calculated as follows:

$$DC(x_d) = \hat{x}_c + \frac{(x_d - \hat{x}_c)}{||x_d - \hat{x}_c||_2} \cdot r_u(||x_d - \hat{x}_c||_2) \ . \tag{1}$$

$$D(x_u) = \hat{x}_c + \frac{(x_u - \hat{x}_c)}{||x_u - \hat{x}_c||_2} \cdot r_u^{-1}(||x_u - \hat{x}_c||_2) \ . \tag{2}$$

$||x - \hat{x}_c||_2$ (in the following r) is the distance (radius) of the point x from the center of distortion $\hat{x}_c$. The function r_u defines for a radius r in the distorted image, the new radius in the undistorted image (for distortion (D), the inverse function r_u^{-1} is required):

$$r_u(r) = \frac{r}{1 + \xi \cdot r^2} \ . \tag{3}$$

This approach is very robust, as only the parameters $\hat{x}_c$ and ξ have to be estimated.

2.2 Traditional Distortion Correction in Feature Extraction

In recent studies [1–3], first the undistorted image I_u is computed from the distorted image I_d. Intuitively, for each point x_u in the undistorted image, the corresponding point x_d in the distorted image must be known. However, as $I_d(x_d)$ exists only for discrete points, the simple assumption $I_u(x_u) = I_d(D(x_u))$ does not hold in general (as $D(x_u)$ not necessarily is a discrete point).

First, a continuous signal $I_{d_{cont}}$ must be generated from I_d by e.g. a linear interpolation method:

$$I_{d_{cont}}(x) = \sum_{z \in N} I_d(z) \cdot K(x - z) \ . \tag{4}$$

N is a set of discrete neighbors of x and K is an arbitrary interpolation kernel. Having the continuous signal, the undistorted image can be computed as follows:

$$I_u(x_u) = I_{d_{cont}}(D(x_u)) \ . \tag{5}$$

The distortion corrected feature extraction is executed in the traditional way, based on the undistorted image I_u.

2.3 Intrinsic Distortion Correction

In the tradition approach, before the feature extraction is applied, the undistorted image is generated. Thereby, the feature extraction can be executed in the usual way, as in the new image the rasterization is retrieved. We introduce a feature extraction methodology with intrinsic DC, which is not based on a re-rasterization.

The main idea of intrinsic distortion correction is explained in the following. We introduce two operations, which preserve geometrical correctness, although pixel values are extracted from the distorted image.

Let x_d be a reference point in the distorted image and v be an arbitrary offset vector. $x_d \oplus v$ adds a vector to a point in the image in consideration of geometrical correctness. Both, the original and the resulting point are coordinates of the distorted image:

$$x_d \oplus v = D(DC(x_d) + v) \ . \tag{6}$$

Otherwise, if two distorted reference points x_{d_1} and x_{d_2} are given, the geometrically correct offset vector can be computed as follows:

$$x_{d_1} \ominus x_{d_2} = DC(x_{d_1}) - DC(x_{d_2}) \ . \tag{7}$$

Using these two operations, each feature can be extracted, theoretically. However, although even a regular grid could be created by adding discrete offset vector ($v = (0,1), (1,1), (1,0), (0,2)...$) to a reference point, intrinsic feature extraction is only sensible if a regular grid is not required. If a grid was essential, interpolation would be necessary in the same way as with the traditional DC.

Features Many features are based on regular grids (e.g. Fourier based and wavelet based features). We identified the following features, being not based on regular grids:

- Local binary patterns [8] (**LBP**)
- Local ternary patterns [9] (**LTP**)
- Rotational invariant Local binary patterns [10] (**RLBP**)

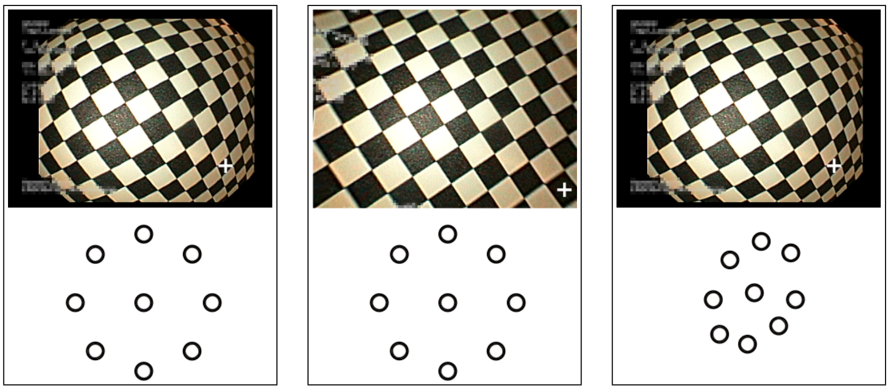

(a) Without DC: Feature extraction based on distorted images with a regular LBP operator.

(b) Traditional DC: Feature extraction based on undistorted images with a regular LBP (Sect. 2.2).

(c) Intrinsic DC: Feature extraction based on distorted images, with a distorted LBP operator (Sect. 2.3).

Fig. 1: The three different feature extraction methodologies are illustrated with a checkerboard image. The top column shows the utilized images and the bottom column shows the applied enlarged LBP templates at the marked point (+).

For computing these features, each (reference) point is encircled by a given number of equidistant circularly arranged samples with a defined radius. The important thing is, that the exact positions of the samples do not necessarily comply with a regular image raster. That means, in each case, interpolation in feature extraction is required. If the traditional DC approach is utilized, interpolation is applied twice (in rasterization and in feature extraction). With our intrinsic approach, one interpolation step can be avoided. We exploit the operation $\oplus$, to get the neighboring points for each center patch, by adding vectors v with a specific length (which is the radius of LBP) and different directions (directly from the original image).

In Fig. 1, the approaches based on the distorted (Fig. 1a) and undistorted images (Fig. 1b) and the intrinsic approach (Fig. 1c) are illustrated.

Whereas most texture features are based on regular grids new features could be developed which directly exploit the operations $\oplus$ and $\ominus$. Moreover, existing features which are based on regular grids can be modified.

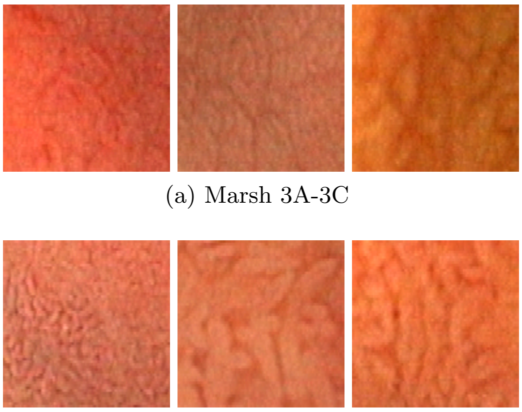

(a) Marsh 3A-3C

(b) Marsh 0

Fig. 2: Example patches of patients with (a) and without the disease (b). In Fig. 2a, the villous structure (b) is missing and only blood vessels can be seen.

3 Experiments

3.1 Experimental Setup

The image test set used contains images of the Duodenal Bulb taken during duodenoscopies at the St. Anna Children's Hospital using pediatric gastroscopes (with resolution 768×576 and 528×522 pixels, respectively). The mean age of the patients undergoing endoscopy was 11.1 years (range 0.8-20.9 years). The female to male ratio was 1.43:1. In a preprocessing step, texture patches with a fixed size of 128×128 pixels were extracted in a manual fashion (examples are shown in Fig. 2). This size turned out to be optimally suited in earlier experiments on automated celiac disease diagnosis [11]. In case of traditional distortion correction, the patch position is adjusted according to the distortion function. With the intrinsic distortion correction, the original patches are preserved. In traditional distortion correction, as well as in feature extraction, bi-linear interpolation is utilized. In our experiments, for feature extraction the patches are converted to gray value images.

To generate the ground truth for the texture patches used, the condition of the mucosal areas covered by the images was determined by histological examination of biopsies from the corresponding regions. Severity of villous atrophy was classified according to the modified Marsh classification in [12].

Although it is possible to distinguish between the different stages of the disease (called Marsh 3A-3C), we only aim in distinguishing between images of patients with (Marsh3A-3C) and without the disease (called Marsh0). Our experiments are based on a database containing 163 (Marsh 0) and 124 (Marsh 3A-3C) images, respectively. As we do not have a separate evaluation set, leave-one-patient-out cross validation is utilized. Thereby we also do not apply any feature subset selection, but instead evaluate various setups with the features mentioned above. For classification, the k-nearest neighbor classifier is used. We utilize this rather simple classifier in order to focus on the feature extraction stage.

3.2 Results

In Fig. 3a - 3c, the results of our Experiments are shown. In each plot for one feature and each configuration (applied on the x-axis), 2 bars are shown. A configuration consists of the radius (first value which is reaching from 1 to 4 pixels) and the number of samples (second value which is reaching from 4 to 10). The bold vertical lines separate the considered radii. Whereas the dark-colored left bars indicate the differences of the classification rates between the intrinsic DC approach and the traditional DC approach, the light-colored right bars indicate the differences between the intrinsic DC and the original approach without distortion correction. A positive value means that the classification rate of the new intrinsic method is higher compared to the other method. The value on top of each column shows the classification rate achieved with the original approach without DC. Adding the respective difference, the absolute classification rates of the intrinsic DC method can be estimated. It can be seen, that the left (dark-colored) bars are almost always above zero. That means, the classification rate definitely benefits from our new intrinsic DC approach compared to the traditional DC approach. The behavior of the right (light-colored) bars seems to depend on the considered neighborhood (i.e. the radius). If radius 1 is chosen, intrinsic DC is disadvantageous compared to the approach without DC for each feature and each number of samples. However, in case of larger neighborhoods (especially if radius is 3 or 4), the intrinsic DC turns out to be the better choice as far as the classification rate is concerned. The overall best achieved classification rates for each feature and each DC method are shown in Table 1.

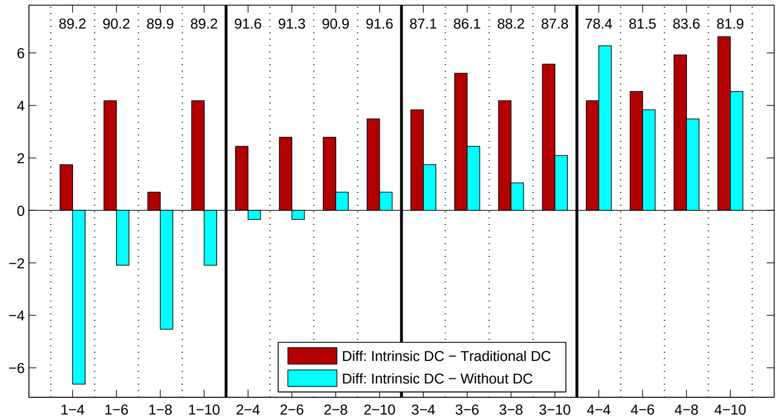

(a) Classification rates achieved with LBP.

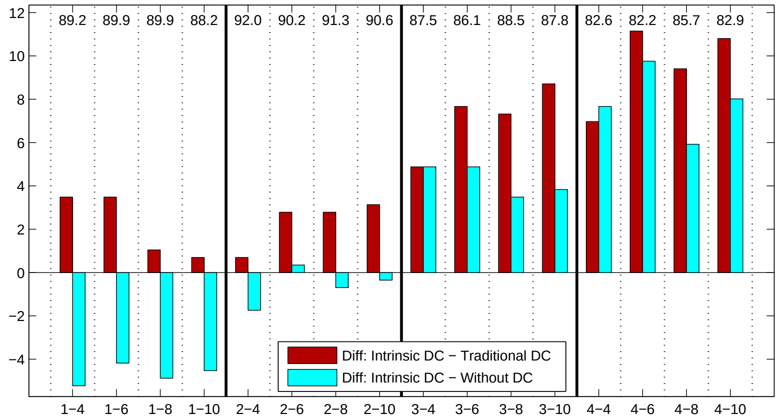

(b) Classification rates achieved with LTP.

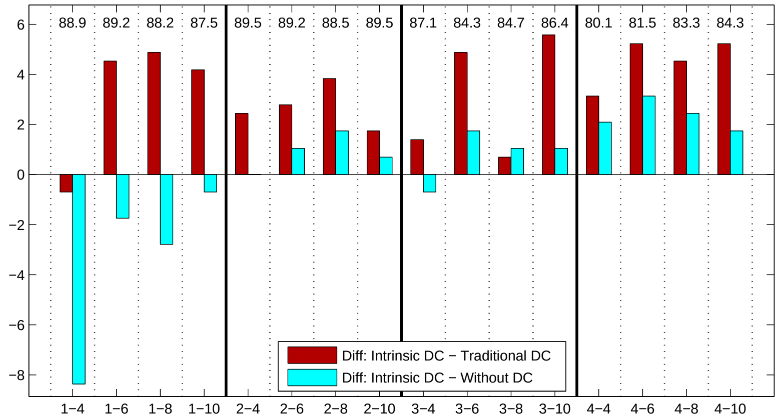

(c) Classification rates achieved with RLBP.

Fig. 3: Classification rates achieved with the different features.

Table 1: Best configurations for each feature and each DC method.

Feature	DC Method	Radius	Samples	Rate
LBP	Without DC	2	8	91.64
	Traditional DC	2	10	88.85
	Intrinsic DC	2	10	**92.33**
LTP	Without DC	2	4	91.99
	Traditional DC	2	4	89.55
	Intrinsic DC	3	4	**92.33**
RLBP	Without DC	2	4	89.55
	Traditional DC	2	6	87.46
	Intrinsic DC	2	8	**90.24**

3.3 Discussion

The new intrinsic DC method definitely is superior to the traditional DC approach. The omitted additional interpolation within rasterization improves the classification rate in nearly each case, especially if larger radii are considered. In comparison with the approach based on the original image, the intrinsic DC approach profits from larger radii. If larger radii are considered, the geometrical correctness takes precedence over the lack of data points. In opposite if small radii are considered, the geometrical (in)correctness has less impact than the missing data points. For an extended discussion on the impact of lens distortion correction on feature extraction and following classification we refer to [5]. With 3 out of the 3 tested features, the best overall classification rates are achieved with the intrinsic DC method.

4 Conclusion

With the introduced distortion correction intrinsic feature extraction, the rasterization which is applied in traditional distortion correction can be omitted for specific features. We show, that the classification rate of celiac disease images benefits from the better preservation of information. A benefit is achieved on the one hand if compared to the traditional DC approach. On the other hand, compared with the approach based on original images, intrinsic DC is advantageous especially if larger neighborhoods are considered. This is an incentive for developing more features which are not based on a regular raster.

Acknowledgment This work is partially funded by the Austrian Science Fund (FWF) under (Project No. 24366).

References

1. Liedlgruber, M., Uhl, A., Vécsei, A.: Statistical analysis of the impact of distortion (correction) on an automated classification of celiac disease. In: Proceedings of the 17th International Conference on Digital Signal Processing (DSP'11), Corfu, Greece (July 2011)
2. Gschwandtner, M., Liedlgruber, M., Uhl, A., Vécsei, A.: Experimental study on the impact of endoscope distortion correction on computer-assisted celiac disease diagnosis. In: Proceedings of the 10th International Conference on Information Technology and Applications in Biomedicine (ITAB'10), Corfu, Greece (November 2010)
3. Gschwandtner, M., Hämmerle-Uhl, J., Höller, Y., Liedlgruber, M., Uhl, A., Vécsei, A.: Improved endoscope distortion correction does not necessarily enhance mucosa-classification based medical decision support systems. In: Proceedings of the IEEE International Workshop on Multimedia Signal Processing (MMSP'12). (September 2012) 158–163
4. Hämmerle-Uhl, J., Höller, Y., Uhl, A., Vécsei, A.: Endoscope distortion correction does not (easily) improve mocusa-based classification of celiac disease. In: Medical Image Computing and Computer-Assisted Intervention – MICCAI 2012. Volume 7512 of Springer Lecture Notes in Computer Science. (September 2012) 574–581
5. Gadermayr, M., Liedlgruber, M., Uhl, A., Vécsei, A.: Evaluation of different distortion correction methods and interpolation techniques for an automated classification of celiac disease. Computer Methods and Programs in Biomedicine (2013) accepted.
6. Melo, R., Barreto, J.P., Falcao, G.: A new solution for camera calibration and real-time image distortion correction in medical endoscopy-initial technical evaluation. IEEE Trans Biomed Eng. **59**(3) (2012) 634–44
7. Fitzgibbon, A.W.: Simultaneous linear estimation of multiple view geometry and lens distortion. In: CVPR. (2001) 125–132
8. Ojala, T., Pietikäinen, M., Harwood, D.: A comparative study of texture measures with classification based on feature distributions. Pattern Recognition **29**(1) (January 1996) 51–59
9. Tan, X., Triggs, B.: Enhanced local texture feature sets for face recognition under difficult lighting conditions. In: Analysis and Modelling of Faces and Gestures. Volume 4778. (October 2007) 168–182
10. Ojala, T., Pietikäinen, M., Mäenpää, T.: Multiresolution Gray-Scale and rotation invariant texture classification with local binary patterns. IEEE Transactions on Pattern Analysis and Machine Intelligence **24**(7) (July 2002) 971–987
11. Hegenbart, S., Kwitt, R., Liedlgruber, M., Uhl, A., Vécsei, A.: Impact of duodenal image capturing techniques and duodenal regions on the performance of automated diagnosis of celiac disease. In: Proceedings of the 6th International Symposium on Image and Signal Processing and Analysis (ISPA '09), Salzburg, Austria (September 2009) 718–723
12. Oberhuber, G., Granditsch, G., Vogelsang, H.: The histopathology of coeliac disease: time for a standardized report scheme for pathologists. European Journal of Gastroenterology and Hepatology **11** (nov 1999) 1185–1194